DOI: 10.19884/j.1672-5220.202501010

Synthesis of PEG-Modified PET Masterbatch: Preparation of Low-Temperature Easy-Dyeing, High-Fastness PET Fibers Based on Phase Domain Size Regulation

XIAO Yongbing[1], XU Chaochen[1], SHEN Wufeng[1], ZHANG Shengming[1], CHEN Xiangling[1], JI Peng[2*], WANG Chaosheng[1], WANG Huaping[1]

1. State Key Laboratory of Advanced Fiber Materials, College of Materials Science and Engineering, Donghua University, Shanghai 201620, China
2. Innovation Center for Textile Science and Technology, Donghua University, Shanghai 201620, China

Abstract: Polyethylene terephthalate (PET) fibers are the largest category of chemical fibers and are widely used. However, the dyeing of PET fibers requires high temperature and pressure (130 ℃ and 0.2 MPa), and the dyeing process consumes huge amounts of energy. Existing studies have shown that the dyeing ability of PET is directly related to the size of the amorphous region, which determines the external conditions for dyeing. In this research, we synthesized a series of low-temperature easy-dyeing masterbatches, PET-co-polyethylene glycol (PETEG), using polyethylene glycol (PEG) with different number-average molecular masses $\overline{M}_n$ and additive amounts. The phase domain size of the amorphous region of PET fibers was regulated via the masterbatch method. The relationship between the phase domain size and dyeing performance was explored from three perspectives: the amount of masterbatch, type of masterbatch, and PEG relative molecular mass. The results indicate that the fiber sample with PEG ($\overline{M}_n$ = 2 000 g/mol) at a mass fraction of 20% modified masterbatch has a smaller crystalline lamellar thickness (5.59 nm) and a larger interlamellar amorphous layer thickness (6.43 nm). The increase in the long period and lamellar inclination angle results in a looser structure, allowing small molecule dyes to diffuse into the fibers more easily. The dye-uptake increases from 63.21% to 92.66% at 100 ℃ with the addition of the masterbatch. Additionally, the dye-uptake of the modified fibers increases with the relative molecular mass of PEG and the mass fraction of the masterbatch. All modified fibers achieve a staining color fastness of grade 4 or higher. This research demonstrates a simple masterbatch method that enables atmospheric pressure dyeing and provides a practical solution for efficient, low-temperature, and low-energy dyeing of PET fibers.

Keywords: polyethylene terephthalate (PET) fiber; polyethylene glycol (PEG); low-temperature dyeing; phase domain size; dye-uptake; color fastness

CLC number: TQ342+.94 **Document code**: A

Article ID: 1672-5220(2025)06-0606-14

Open Science Identity (OSID)

0 Introduction

Polyethylene terephthalate (PET) fibers are cost-effective, accounting for over 75% of global chemical fiber production[1]. However, the regularity of the chemical structure and the high glass transition temperature T_g limit dyeing options to disperse dyes, which require high temperature (130 ℃) and high pressure (0.2 MPa). The dyeing of PET fibers is energy-intensive, with long dyeing time and low dye utilization. Furthermore, various dyeing auxiliaries are required. Dyeing process optimization or efficiency improvement is urgently needed. To reduce energy consumption and achieve low-carbon dyeing for PET fibers, modifying the PET fibers is essential[2].

The poor dyeing properties of PET fibers can be attributed to two main factors[3-4]. First, the regular and compact molecular structure of PET, characterized by high crystallinity, hinders the diffusion of dye molecules into its interior. Besides, PET molecules contain fewer polar groups, resulting in weaker intermolecular forces with dyes.

To improve the dyeing properties of PET fibers, existing research focuses on improving dyeing methods and modifying the PET molecular structure. Methods for producing colored PET fibers include carrier dyeing[5] and in-situ coloring[6]. However, to fundamentally solve the high-temperature and high-pressure dyeing conditions of PET fibers, the molecular structure of PET needs to be optimized. Existing studies have been carried out by introducing a third and fourth monomer into PET. Examples include long-chain polyethers[7], isophthalic acid (IPA)[8], adipic acid (AA)[9], and sodium-5-sulfo-bis(hydroxyethyl)-isophthalate (SIPE)[10-12]. Among all

Received date: 2025-01-18

Foundation item: Key R&D Program of the Xinjiang Uygur Autonomous Region, China (No. 2024B01011)

* Correspondence should be addressed to JI Peng, email: jipeng@dhu.edu.cn

Citation: XIAO Y B, XU C C, SHEN W F, et al. Synthesis of PEG-modified PET masterbatch: preparation of low-temperature easy-dyeing, high-fastness PET fibers based on phase domain size regulation[J]. *Journal of Donghua University (English Edition)*, 2025, 42(6): 606-619.

the modified monomers, long-chain polyether modification is dominant. Incorporating long-chain polyether enhances the mobility of the molecular chains, leading lower T_g [13-15]. Furthermore, the introduction of long-chain polyether disrupts the regular arrangement of PET molecules, thereby reducing crystallinity. Polyethylene glycol (PEG), a derivative of aliphatic long carbon chains, exhibits good flexibility, which helps reduce both the crystallinity and T_g of PET. Furthermore, the ether bonds in PEG contribute a degree of polarity, enhancing the hydrophilicity of PET[13,16]. These make PEG an ideal monomer for modifying PET via copolymerization.

Studies have shown that the copolymerization modification method positively affects the dyeing performance of PET. However, to further improve dyeing effectiveness, a deeper investigation into the microstructure of PET is necessary. The masterbatch method combines chemical copolymerization with physical mixing. It involves preparing a concentrate by dispersing functional substances into a carrier resin, which is subsequently diluted with the primary matrix resin in a specific ratio to form the final product[12]. The masterbatch method has a more multidimensional way of adjusting the distribution of soft segments compared with the traditional direct copolymerization modification. The phase domain size of the amorphous region can be flexibly adjusted by masterbatch copolymerization and blend modification, which helps to study the relationship between the phase domain size and dyeing properties.

In this study, the effect of the masterbatch addition on the dyeing properties of PET fibers was investigated in terms of the amount of masterbatch, type of masterbatch (which affects the PEG distribution in the amorphous region), and PEG relative molecular mass. A series of easy-dyeing masterbatches was prepared by direct esterification polymerization. The fibers were further prepared by melting spinning through the masterbatch method, and the mechanical properties, crystalline properties, and dyeing properties were investigated. The size of the amorphous region of the fibers and the microcrystalline structure were also analyzed by small-angle X-ray scattering (SAXS), which was successfully linked to the changes in the dyeing properties of the fibers.

1 Materials and Methods

1.1 Materials

Terephthalic acid (PTA, industrial grade) was obtained from Sinopec Yangzi Petrochemical Co., Ltd., China. Ethylene glycol (EG) and antimony glycolate ($Sb_2(OCH_2CH_2O)_3$) were purchased from Sinopharm Chemical Reagent Co., Ltd., China. PEG, with $\overline{M}_n$ of 1 000, 2 000 and 4 000 g/mol, respectively, was purchased from Shanghai Yuanye Biotechnology Co., Ltd., China. Triphenyl phosphite (TPPi) was purchased from Shanghai Aladdin Biochemical Technology Co., Ltd., China. Phenol, 2, 2, 4, 4-tetrachloroethane, hexafluoro isopropanol (HFIP), and trifluoroacetic acid-d (TFA-d_1) were purchased from Sigma-Aldrich (Shanghai) Trading Co., Ltd., China. Fiber-grade PET pellets were purchased from Poly Plastic Masterbatch (Suzhou) Co., Ltd., China. Dispersed deep blue-HGL was purchased from Zhejiang Longsheng Group Co., Ltd., China.

1.2 Preparation

1.2.1 Preparation of low-temperature dyeing PET masterbatch

A series of low-temperature dyeing PET masterbatches was prepared, denoted as $PETEG_{x\text{-}y}$, where x indicates the $\overline{M}_n$ of PEG and y indicates the amount of PEG added. For instance, $PETEG_{2k\text{-}6}$ is defined as a masterbatch containing a mass fraction of 6% PEG-2000. PETEG was synthesized through direct esterification, as illustrated in Fig. 1. PTA (18.0 mol), EG (21.6 mol), $Sb_2(OCH_2CH_2O)_3$ (1.20 g), and TPPi (1.20 g) were added to a 10 L stainless steel reactor and heated to 220 ℃ under a nitrogen atmosphere. The system pressure was maintained at 0.6 MPa and slowly relieved, with the reaction lasting 3 h. When the water conversion reached 95% of the theoretical value, the reaction mixture was heated to (270±3) ℃ under high vacuum (<50 Pa), and polycondensation was carried out. The reaction ended when the mixing power reached a predetermined value. All samples were used directly for characterization without purification.

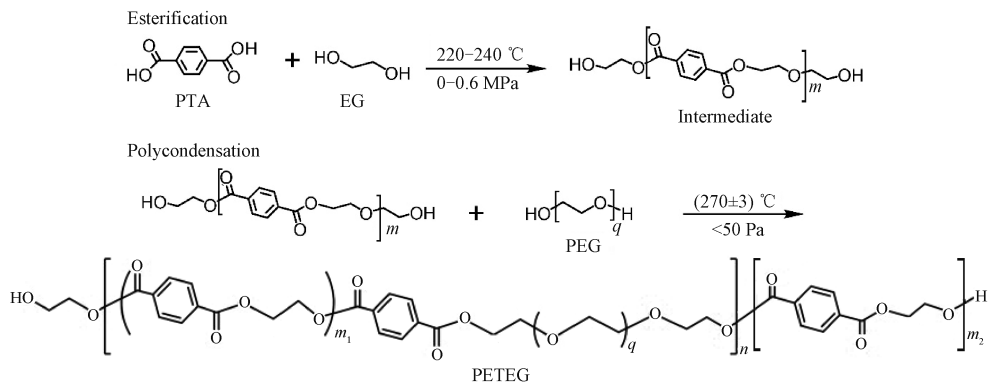

Fig. 1 Synthesis route of PETEG

1.2.2 Preparation of low-temperature dyeing PET slices and fibers

The low-temperature dyeing PET slices named SPETEG$_{x\text{-}y}$-z% were prepared by melt blending the masterbatch with PET. The masterbatch-modified fibers were named as FPETEG$_{x\text{-}y}$-z%. Here, S denotes that the sample is in slice form, and F denotes that the sample is in fiber form. PETEG$_{x\text{-}y}$ indicates the type of masterbatch, and z represents the amount of masterbatch added. For example, FPETEG$_{2k\text{-}6}$-30.0% represents the fiber prepared by a mass fraction of 30.0% PETEG$_{2k\text{-}6}$.

1.3 Characterization and testing

1.3.1 Color value testing

A spectrophotometer (S81, Truss, USA) was used to measure the b value (a yellowness-blueness index) of the masterbatch by selecting the masterbatch mode, the light source was selected to be D65 light source, and the observer angle was selected to be 10°.

1.3.2 Intrinsic viscosity and molecular mass testing

The intrinsic viscosity $[\eta]$ of PETEG was measured in the solvent of phenol and 1,1,2,2-tetrachloroethane (a mass ratio of 1∶1) by a viscometer in the water bath at 25 ℃. The weight-average molecular mass $\overline{M}_w$, $\overline{M}_n$, and polydispersity index $Đ$ were characterized by gel permeation chromatography (GPC) using an Agilent 1260 Infinity Ⅱ system (Agilent, USA). The measurements were conducted at 35 ℃.

1.3.3 Molecular structure characterization

The characteristic functional groups were measured by attenuated total reflectance Fourier transform infrared (ATR-FTIR) (Nicolet 6700, Nicolet, USA). The scanning wavenumber was 600 – 4 000 cm^{-1}, and the number of scans was 32. The prepared low-temperature dyeing masterbatch was extracted by Soxhlet extraction (the extraction solvent was trichloromethane, and the extraction temperature was 105 ℃). The molecular structures were characterized by ^{1}H nuclear magnetic resonance (^{1}H-NMR) spectroscopy using a Bruker AVANCE Ⅲ HD 600 spectrometer (Bruker, Germany).

1.3.4 Thermal property characterization

The melting and crystallization behaviors of PET and PETEG were characterized by a differential scanning calorimeter (DSC) (Q20, TA, USA) under a nitrogen atmosphere. The heating and cooling rates were 10 ℃/min. The thermal stability of PET and PETEG was investigated by thermogravimetric analysis (TGA), and the measurements were performed on a TG209F3 instrument (Netzsch, Germany). The sample (5 – 10 mg) was heated from 25 to 550 ℃ at a rate of 10 ℃/min under a nitrogen atmosphere.

1.3.5 Hydrophilic property characterization

The low-temperature dyeing PET slices were injection molded into 2.5 cm diameter discs by vertical injection molding, and the hydrophilicity of the low-temperature dyeing PET slices was tested by using a Theta T200 contact angle meter (Biolin Scientific, Finland). The test liquid was deionized water, with a droplet volume of 3 mL each time.

1.3.6 Crystal structure characterization

A wide-angle X-ray diffractometer (WAXD) (BL14B1, SSRF, China) was used to characterize the crystalline properties of the modified fibers. LaB_6 was used as the standard sample, and the distance from the calibration sample to the detector was 248.4 mm. SAXS tests were performed at the BL16B1 beam station at the Shanghai Light Source (SSRF), China, where SAXS data were collected by using a Mar CCD 165. The wavelength of the X-ray was 0.124 nm, and the distance from the calibration sample to the detector was 2 450 mm.

1.3.7 Dynamic thermomechanical (DMA) property characterization

The DMA curves of the fiber samples were collected by using a dynamic mechanical analyzer (Q850, TA Instruments, USA) from 0 to 120 ℃ at a 1 Hz tensile frequency under a nitrogen atmosphere.

1.3.8 Mechanical property testing

Mechanical properties of the fibers were tested by using an XL-1 type compound filament strength elongation instrument (Shanghai New Fiber Instrument Co., Ltd., China), with a clamping distance of 200 mm and a tensile rate of 250 mm/min. The average value was taken from several measurements.

1.3.9 Dyeing performance testing

The fibers were washed to remove surface oils before dyeing. The dispersed deep blue-HGL dye solution at a bath ratio of 1∶20 and a dye dosage of 8% on the mass of fiber (omf) was prepared. The modified fibers were dyed by using an infrared dyeing machine (Xiamen Ruibi Co., Ltd., China) at dyeing temperatures of 90, 100, 110, 120, and 130 ℃, respectively, and the dyeing time of 40 min. The stained samples were reduced and washed at 50 ℃ for 20 min in an aqueous solution containing NaOH and $Na_2S_2O_4$ (2 g/L), with a bath ratio of 1∶50. The dye-uptake was determined according to GB/T 9337—2009 standard, and the K/S value was measured by a colorimeter under a D65 light source at 10°.

2 Results and Discussion

2.1 Intrinsic viscosity and molecular mass

The conventional properties of PETEG are shown in Table 1.

As shown in Table 1, the intrinsic viscosity of PETEG increases with the PEG mass fraction. This is because the introduction of PEG decreases the melt viscosity of the PET. To achieve the same stirring current as unmodified PET, a longer reaction time is required for the polymerization process. This extended polycondensation time, in turn, allows for an increase in the molecular chain length.

Table 1 Conventional properties of PETEG

Masterbatch	$\overline{M}_n$	$\overline{M}_w$	$Đ$	$[\eta]$/(dL/g)	b value
$PETEG_{2k-6}$	18 579	39 573	2.13	0.67	9.16
$PETEG_{2k-12}$	20 504	42 033	2.05	0.72	10.95
$PETEG_{2k-24}$	24 453	56 730	2.32	0.83	9.62
$PETEG_{1k-20}$	24 273	40 293	1.66	0.83	11.41
$PETEG_{2k-20}$	23 774	50 163	2.11	0.81	11.08
$PETEG_{4k-20}$	24 095	45 298	1.88	0.82	12.86

2.2 Molecular structure

ATR-FTIR spectra were utilized to detect the structures of PET and PETEGs. The results are shown in Figs. 2(a) and 2(b). In Fig. 2(a), the distinct peak at 1 750 cm^{-1} is observed due to the C═O stretching vibration. The peaks at 1 100 and 1 265 cm^{-1} are attributed to the symmetric and asymmetric stretching vibrations of the C—O bond, indicating the formation of the ester bond. The peak at 1 410 cm^{-1} is attributed to the stretching vibration of the aryl ring backbone. Figure 2(b) is a partial magnification of the ATR-FTIR spectra at around 2 880 cm^{-1}, the vibrational peaks are caused by the $—CH_2$ stretching vibration of PEG[17]. The distinct characteristic peak of PETEG at 2 880 cm^{-1} indicates that PEG has been successfully copolymerized into the molecular chain. Figure 2(c) shows the ^{1}H-NMR spectrum of the masterbatch after Soxhlet extraction with $CHCl_3$. Peak 1 is the H peak on the benzene ring and appears at 8.05. Peak 2 is the H peak on the ethylene glycol methylene group and appears at 4.75. Peak 3 is the H peak on the PEG methylene group. Peaks 4 and 5 are the methylene ends of PEG[18].

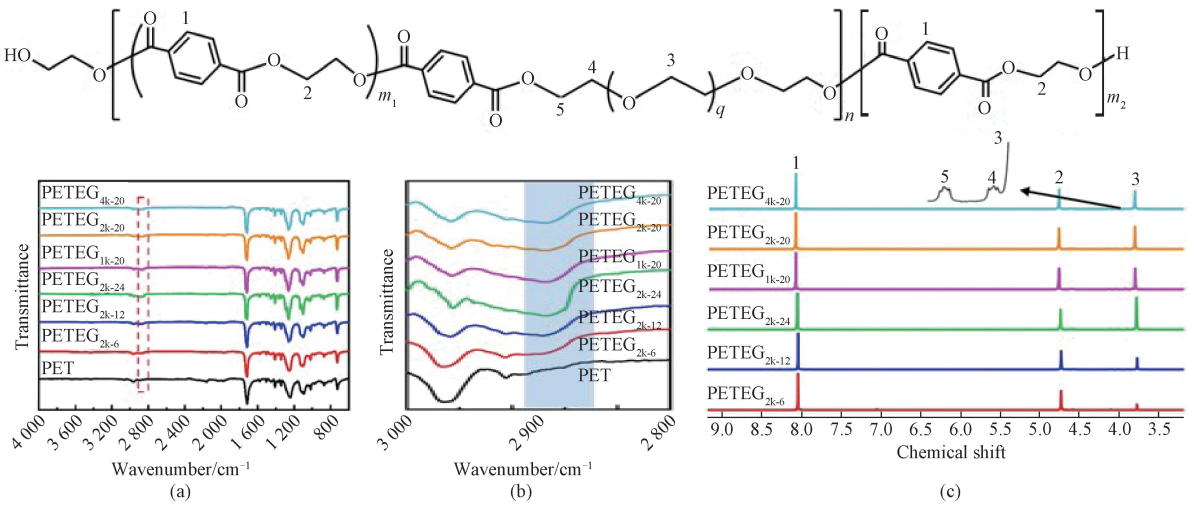

Fig. 2 Chemical structure of PET and PETEGs: (a) ATR-FTIR spectra; (b) $—CH_2$ stretching vibrational peaks; (c) ^{1}H-NMR spectra of PETEGs

The mass fraction of PEG $W_{(PEG)}$ can be calculated according to Ref. [19] by

$$W_{(PEG)} = \frac{I_3/4 \times 44}{I_1/4 \times 192 + I_3/4 \times 44}, \quad (1)$$

where I_1 is the intensity of peak 1 in Fig. 2(c); I_3 is the intensity of peak 3 in Fig. 2(c).

The mass of the PEG chain segments versus the PET chain segments M_{soft}/M_{hard} in the co-polyester masterbatch can be calculated according to Ref. [19] by

$$M_{soft}/M_{hard} = \frac{I_3 \times M_{(PEG)}}{I_1 \times M_{(PET)}}, \quad (2)$$

where $M_{(PEG)}$ and $M_{(PET)}$ are the relative molecular masses of PEG and PET, respectively.

When a small amount of PEG is added, not every molecular chain contains PEG segments. The average number of PEGs per molecular chain $n_{(PEG)}$ can be calculated as

$$n_{(PEG)} = \frac{M_{n(PETEG)} \times W_{(PEG)}}{M_{n(PEG)}}, \quad (3)$$

where $M_{n(PETEG)}$ represents the number-average molecular mass of PETEG, $M_{n(PEG)}$ represents the number-average molecular mass of PEG.

The average number of PET segments per molecular chain, denoted as $L_{(PET)}$, can then be calculated according to Ref. [20] by

$$L_{(PET)} = \frac{M_{n(PETEG)} \times W_{(PET)}}{n_{(PET)} \times M_{(PET)}}, \quad (4)$$

where $W_{(PET)}$ represents the mass fraction of PET in PETEG; $n_{(PET)}$ is the average number of PET segments per molecular chain.

Table 2 summarizes $n_{(PEG)}$ and $L_{(PET)}$ for PETEG

samples. When $n_{(PEG)}$ is less than 1 mol, the distribution of PEG along the molecular chains is heterogeneous, resulting in some chains lacking PEG segments. When $W_{(PEG)}$ increases and the relative molecular mass of PEG decreases, $L_{(PET)}$ decreases. This is because, for a given mass, a PEG with a lower number-average molecular mass possesses a higher number of polymer chains, and consequently, more terminal hydroxyl groups. These hydroxyl groups act as additional reaction sites during esterification with the prepolymer. By reacting with the prepolymer, they effectively terminate the chain growth, leading to a shorter average chain length.

Table 2 Structural parameters of PETEGs

Masterbatch	$W_{(PEG)\text{-theory}}$/%	$W_{(PEG)}$/%	M_{soft}/M_{hard}	$n_{(PEG)}$/mol	$L_{(PET)}$
$PETEG_{2k\text{-}6}$	6	5.61	0.059	0.559	58.59
$PETEG_{2k\text{-}12}$	12	11.01	0.124	1.211	42.98
$PETEG_{2k\text{-}24}$	24	22.68	0.293	2.781	24.34
$PETEG_{1k\text{-}20}$	20	18.46	0.226	4.863	17.58
$PETEG_{2k\text{-}20}$	20	19.62	0.223	2.503	28.41
$PETEG_{4k\text{-}20}$	20	18.73	0.231	1.126	47.97

Note: $W_{(PEG)\text{-theory}}$ represents the theoretical mass fraction of PEG.

2.3 Thermal property

The DSC and TG curves for PET and PETEGs are presented in Fig. 3. The thermal properties of the samples are summarized in Table 3. Figure 3(a) shows the enthalpy change during the cooling crystallization process of the masterbatch. At a PEG mass fraction of 24%, the excessive addition of PEG disrupts the molecular chain regularity, hindering the crystallization process and lowering the crystallization temperature T_c. As the relative molecular mass of PEG increases, the crystallization rate of the masterbatch also increases[21]. Figure 3(b) shows that the melting point T_m shifts from a higher temperature to a lower temperature, and the melting range broadens after the copolymerization of PEG and PET. This is because PEG enhances the flexibility of the macromolecular chains and increases the free volume between them, thereby raising the thermodynamic entropy. Consequently, the melting point T_m decreases[22].

Figure 3(c) shows the heat loss curve of the masterbatch. The initial decomposition temperature $T_{5\%}$ of the sample gradually decreases with increasing PEG content. As the relative molecular mass of PEG increases, the initial decomposition temperature gradually increases. This is because PEG chains with a lower relative molecular mass are shorter and more likely to integrate into PET chains, disrupting their regularity[23]. The initial decomposition temperatures of all masterbatches are above 375 ℃, indicating that they do not interfere with the subsequent processing.

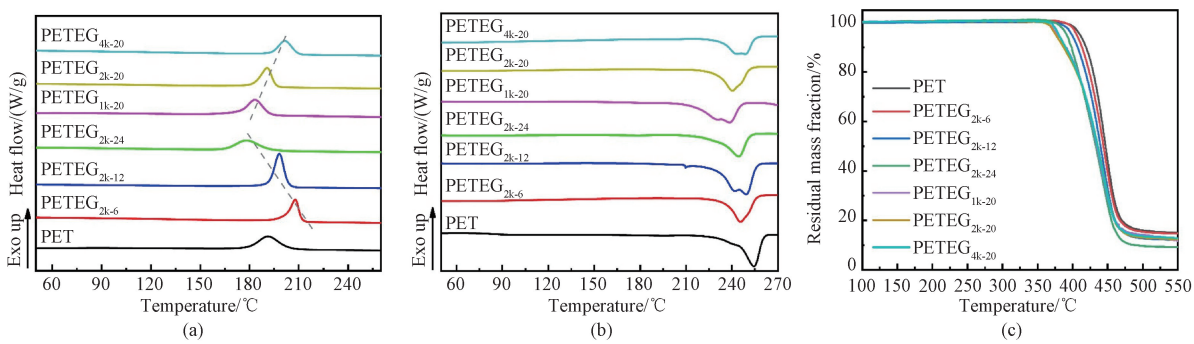

Fig. 3 Thermal properties of PET and PETEGs: (a) DSC first cooling curves; (b) DSC second heating curves; (c) TG curves

Table 3 Thermal performance parameters of PET and PETEGs

Masterbatch	T_c/℃	ΔH_c/(J/g)	T_m/℃	ΔH_m/(J/g)	$T_{5\%}$/℃
PET	191.38	41.24	254.44	39.79	410.56
$PETEG_{2k\text{-}6}$	207.84	39.59	245.70	35.45	405.75
$PETEG_{2k\text{-}12}$	198.16	37.22	244.96	32.92	399.04
$PETEG_{2k\text{-}24}$	178.26	32.09	244.56	29.41	391.54
$PETEG_{1k\text{-}20}$	183.47	30.88	238.61	27.17	375.85
$PETEG_{2k\text{-}20}$	197.33	32.18	240.50	30.53	378.91
$PETEG_{4k\text{-}20}$	201.65	35.07	248.98	31.43	380.13

Note: ΔH_c and ΔH_m represent the crystallization enthalpy and melting enthalpy, respectively.

2.4 Hydrophilic property

Figure 4 depicts the hydrophilicity of the modified PET after masterbatch addition. As can be seen from Figs. 4(a) and 4(b), the water contact angle (WCA) of the modified PET decreases from 86.98° to 52.40° with the increase of the mass fraction of PEG. This is because the PEG contains a large amount of ether bonds, and the ether bonds can form a strong hydrogen bond between the ether and water molecules, which reduces the WCA[24]. Figure 4(c) depicts the WCAs of different types of masterbatch modified PETs, and it can be found that the WCA of $SPETEG_{2k\text{-}6}$-30.0% is 3.2° lower than that of $SPETEG_{2k\text{-}24}$-7.5% with the same ether bond content. The higher addition of the masterbatch with a lower modified content leads to a more homogeneous distribution of the masterbatch in PET and a higher ether bond content on the surface of its samples. In addition, comparing the samples with the addition of the masterbatch modified with different relative molecular masses of PEG, the higher the relative molecular mass of PEG, the better the hydrophilicity of the samples.

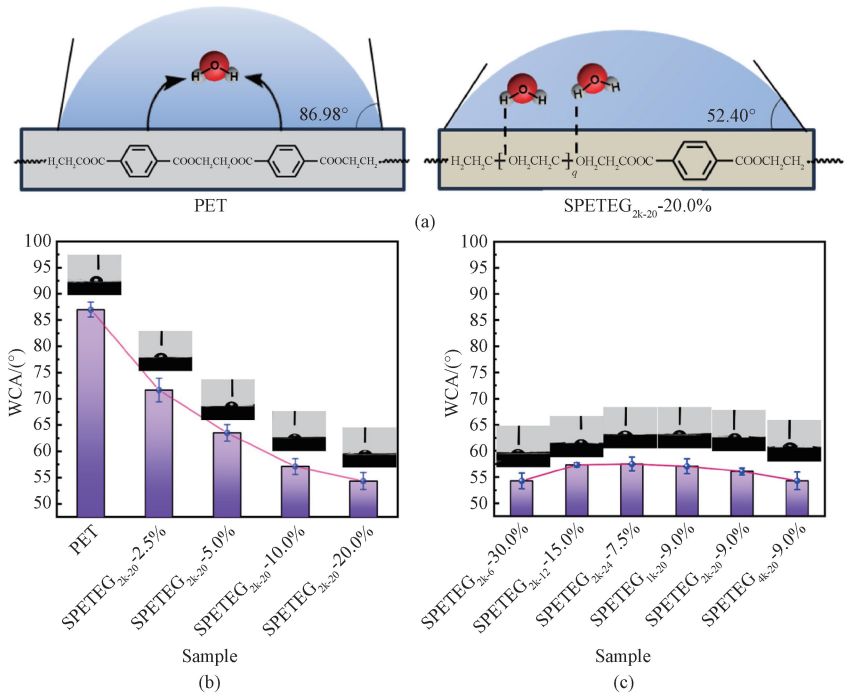

Fig. 4 WCA of PET and SPETEGs: (a) schematic diagram of WCA measurement; (b) different amounts of masterbatches; (c) different types of masterbatches

2.5 Crystal structure

2.5.1 Crystallinity and crystal size

The crystalline properties of the modified PET fibers were analyzed by WAXD. WAXD patterns of FPETEGs with varying contents of $PETEG_{2k\text{-}20}$ masterbatch are shown in Fig. 5(a). The WAXD curves in Fig. 5(b) is obtained by integrating the one-dimensional (1D) WAXD data along the equatorial direction. PET exhibits stronger diffraction peaks in the equatorial direction, and the intensity of these peaks gradually decreases with the addition of $PETEG_{2k\text{-}20}$. The modified PET exhibits distinct diffraction peaks at 14.20°, 17.56°, and 20.08°, corresponding to the crystallographic planes (010), $(\bar{1}10)$, and (100)[25]. These peaks are consistent with those of PET, indicating that the addition of PEG chain segments does not alter the crystal lattice structure.

To investigate the effect of the masterbatch addition on the crystal structure of PET, the crystallinity X_c and crystal size of the samples are calculated according to Refs. [26-27] by

$$X_c = \frac{S_c}{S_c + S_a} \times 100\%, \quad (5)$$

$$L_{hkl} = \frac{K\lambda}{\beta \cos\theta}, \quad (6)$$

where S_c represents the total integral area of crystallisation peaks after peak separation; S_a represents the total integral area of non-crystalline peaks after peak separation; L_{hkl} indicates the average crystal size in the crystal plane direction; $K = 0.89$; $\lambda = 0.154$ nm; β is the half-height width of the diffraction peak; θ is the Bragg angle corresponding to the diffraction peak position.

Figure 5(c) shows the crystallinity and crystal size plots of modified fibers prepared with varying masterbatch mass fractions. The crystallinity decreases from 32.33% to 27.61% as the masterbatch mass fraction increases. This decrease is attributed to the hindrance of PEG chain segments to the regular arrangement of PET chain segments. Figure 5(d) shows the crystallinity and crystal size of modified fibers prepared with different types of masterbatches. The crystallinity of $FPETEG_{2k\text{-}6}$-30.0% is

1.13% lower than that of $FPETEG_{2k\text{-}24}$-7.5%, suggesting that a higher addition of the masterbatch with a lower modification content disrupts the PET crystal structure more severely. The addition of the PEG-modified masterbatch with different relative molecular masses has no significant effect on the crystallinity of PET. Comparison of crystal sizes shows that the masterbatch addition primarily reduces the size of crystallites along the $(\bar{1}10)$ plane, with little effect on the (010) and (100) planes.

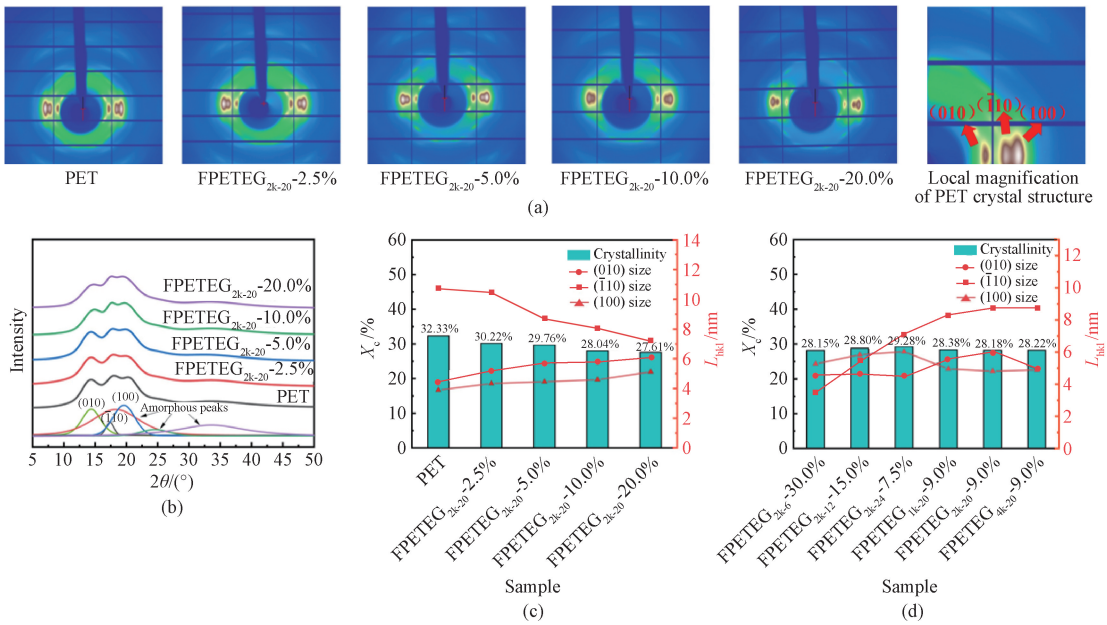

Fig. 5 Crystalline properties of modified fibers: (a) WAXD patterns; (b) WAXD curves; (c) structural parameters for different amounts of masterbatches; (d) structural parameters for different types of masterbatches

2.5.2 Lamellar structure

To further investigate the effect of the masterbatch addition on the lamellar crystal structure and amorphous region size in PET, SAXS characterization was performed on modified PET fibers. Figure 6 shows the two-dimensional (2D) SAXS patterns of samples with varying $FPETEG_{2k\text{-}20}$ additions. All images exhibit two lamellar crystal stripes along the meridian direction, with an equatorial stripe passing through the beamstop. The scattering vector parallel to the fiber axis is defined as $\boldsymbol{q}_1$, and the vector perpendicular to the fiber axis is defined as $\boldsymbol{q}_2$[28]. Scattering peaks on both sides of the beamstop result from the periodic distribution of electron densities in the oriented lamellar crystal structure. Scattering peaks in the meridian direction weaken as the amount of masterbatch addition increases. Additionally, the scattering peaks shift from a two-point mode to a four-point mode, due to the tilting of the lamellar crystals along the fiber axis[29].

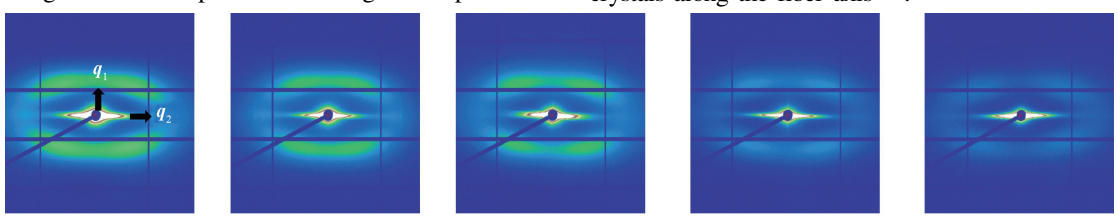

Fig. 6 2D SAXS patterns: (a) PET; (b) $FPETEG_{2k\text{-}20}$-2.5%; (c) $FPETEG_{2k\text{-}20}$-5.0%; (d) $FPETEG_{2k\text{-}20}$-10.0%; (e) $FPETEG_{2k\text{-}20}$-20.0%

Figure 7(a) presents the scattering intensity versus scattering vector plot for the modified PET fibers along the $\boldsymbol{q}_1$ direction. The position of the peak corresponding to the maximum scattering intensity $\boldsymbol{q}_{1\max}$ is recorded, and the long period L of the samples is calculated according to Ref. [30] by

$$L = \frac{2\pi}{\boldsymbol{q}_{1\max}}. \tag{7}$$

The Fourier transform of the 1D scattering intensity distribution yields its corresponding correlation function curve, where Z denotes the distance scale and $\gamma(Z)$ represents the correlation function. Figure 7(b) presents the 1D electron density distribution function for modified PET fibers prepared with different amounts of masterbatches, from which the long period L^*, the average thickness L_a of the interlamellar amorphous layer, and the average thickness L_c of the interlamellar crystalline layer can be determined. Figure 7(c) shows the 1D integration curves for different types of masterbatches. L_a

of $FPETEG_{2k\text{-}6}$-30.0% is 0.21 nm larger than that of $FPETEG_{2k\text{-}24}$-7.5%, while L_c is 0.33 nm smaller. This suggests that the high-additive and low-modification method more effectively suppresses the crystallization of PET, leading to a higher amorphous content. Comparison of the samples prepared with PEG modifiers of different relative molecular masses shows that the $FPETEG_{4k\text{-}20}$-9.0% sample has a larger long period, while L_c remains almost constant.

To examine the variation in the lamellar inclination φ of the lamellar crystals, SAXS plots were integrated along the q_2 direction, as shown in Figs. 7(d) and 7(e). Calculations are performed as

$$\varphi = \arctan\frac{\Delta x}{2q_{2\max}}, \tag{8}$$

where Δx represents the distance between the two peaks on the integrated plot.

Figure 7(f) presents a structure evolution diagram with the masterbatch addition.

The transverse dimension D_{SAXS} of the lamellar crystal layer is calculated as

$$D_{SAXS} = \frac{2\pi}{\Delta q_2}. \tag{9}$$

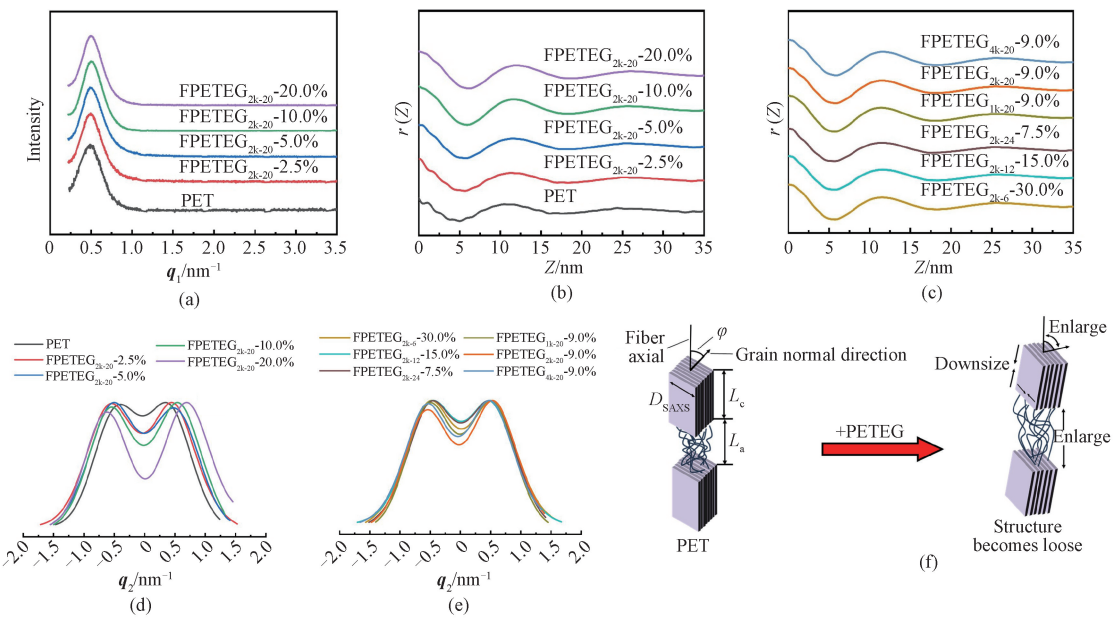

Fig. 7 SAXS images of modified fibers: (a) SAXS along q_1 direction; (b) Fourier transform function along q_1 direction for modified fibers with different amounts of masterbatches; (c) Fourier transform function along q_1 direction for modified fibers with different types of masterbatches; (d) strength of modified fibers along q_2 direction for different amounts of masterbatches; (e) strength of modified fibers along q_2 direction for different types of masterbatches; (f) structure evolution diagram with masterbatch addition

The parameters of the lamellar crystal structure of modified PET fibers are summarized in Table 4.

As shown in Table 4, the addition of the masterbatch results in an increase in the long period L of the samples. This increase suggests a looser stacking of lamellar crystals. When comparing the different amounts of masterbatches, it is observed that the long period of $FPETEG_{2k\text{-}24}$-7.5% is larger than that of $FPETEG_{2k\text{-}6}$-30.0%. Furthermore, the fibers prepared from the masterbatch containing a higher relative molecular mass of PEG exhibit a longer period.

Table 4 Parameters of lamellar crystal structure of modified PET fibers

Sample	L/nm	L^*/nm	L_a/nm	L_c/nm	φ/(°)	D_{SAXS}/nm
PET	12.53	10.95	4.88	6.07	41.17	7.30
$FPETEG_{2k\text{-}20}$-2.5%	12.71	11.31	5.38	5.93	46.83	6.94
$FPETEG_{2k\text{-}20}$-5.0%	12.80	11.48	5.77	5.71	46.94	6.83
$FPETEG_{2k\text{-}20}$-10.0%	12.89	11.53	5.90	5.63	49.44	6.65
$FPETEG_{2k\text{-}20}$-20.0%	12.99	12.02	6.43	5.59	53.74	6.57
$FPETEG_{2k\text{-}6}$-30.0%	12.73	11.51	5.82	5.69	47.15	6.61
$FPETEG_{2k\text{-}12}$-15.0%	12.81	11.56	5.64	5.92	46.17	6.65
$FPETEG_{2k\text{-}24}$-7.5%	12.84	11.63	5.61	6.02	45.87	6.64
$FPETEG_{1k\text{-}20}$-9.0%	12.62	11.33	5.63	5.70	46.24	7.08
$FPETEG_{2k\text{-}20}$-9.0%	12.77	11.56	5.81	5.75	47.21	7.03
$FPETEG_{4k\text{-}20}$-9.0%	12.79	11.71	5.92	5.79	48.58	6.85

The long period L calculated from Bragg's equation is larger than the long period L^* derived from the 1D electron density distribution function. Although the two values differ, their trends are consistent. Here, L^* is selected to calculate L_c, where $L_c = L^* - L_a$. The calculation shows that as the amount of masterbatch increases, L_a increases while L_c decreases, indicating that the crystal structure of the fiber samples becomes more loosely stacked.

When the same type of masterbatch is added, the crystallinity of the lamellar crystal increases with the amount of the masterbatch. Comparing different masterbatches with the same actual PEG content reveals that crystallinity is more significantly affected by two factors: the use of a low-PEG-content masterbatch at a high addition amount, and the use of a masterbatch modified with a high relative molecular mass PEG.

The addition of different types of masterbatches has little effect on D_{SAXS}. The transverse dimension of the lamellar crystal layer depends solely on the actual PEG content in the matrix, decreasing as the PEG content in the modified fiber increases.

2.6 Dynamic thermomechanical property

The glass transition temperature T_g is a key parameter affecting the dyeability of fibers. As shown in Fig. 8, which illustrates the dynamic thermomechanical properties of the modified PET fibers, T_g was determined by DMA through applying a frequency-varying mechanical stress and monitoring the change in the loss tangent ($\tan\delta$). In Fig. 8(a), increasing the amount of masterbatch shifts the α-transition peak of PET to a lower temperature. This occurs because the introduction of PEG disrupts the regular arrangement of PET molecular chains and increases the free volume between chain segments[31]. Figure 8(b) shows that FPETEG$_{2k\text{-}6}$-30.0% exhibits the lowest α-transition temperature. This is attributed to the higher concentration of ether bonds being more uniformly distributed, which more effectively disrupts the regularity of the molecular chain arrangement and consequently leads to a reduction in the overall crystallinity. These observations are consistent with the WAXD results. Figure 8(c) shows the variation of the loss tangent with temperature for modified PET fibers prepared from the masterbatches containing PEGs of different relative molecular masses. The positions of the α-transition peak for fibers modified with different PEG relative molecular masses are approximately the same.

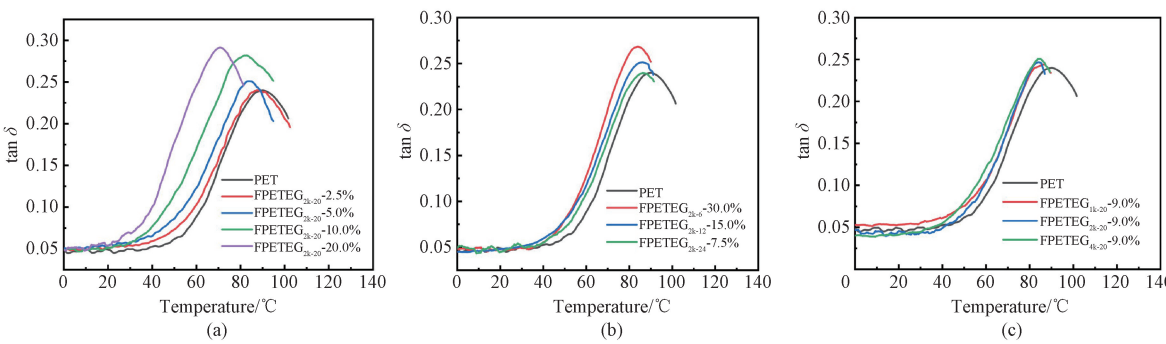

Fig. 8 Curves of tan δ versus temperature for modified PET fibers: (a) different amounts of masterbatches; (b) different types of masterbatches; (c) different relative molecular masses of masterbatches

2.7 Mechanical property

Figure 9(a) shows the mechanical properties of the modified fibers prepared by adding different amounts of masterbatches. As the amount of masterbatch addition increases, the elongation at break of the fiber increases, while the tensile strength decreases. PEG is a flexible chain segment, and the inclusion of PEG enhances the fiber flexibility, which consequently reduces the fiber strength. Furthermore, the PEG molecular chain possesses considerable free volume and length, contributing to increased fiber elongation during the stretching process[10]. Figure 9(b) depicts the mechanical property curves of the modified fibers prepared by adding different types of masterbatches. The FPETEG$_{2k\text{-}6}$-30.0% sample has the lowest tensile strength and the highest elongation at break. This is because the FPETEG$_{2k\text{-}6}$-30.0% sample contains the highest masterbatch mass fraction and the most uniform distribution of PEG flexible chain segments. This uniform distribution greatly destroys the crystallinity of PET and provides more free space for molecular chain movement. Figure 9(c) illustrates the mechanical properties of the modified PET fibers prepared by adding PEG masterbatches with different relative molecular masses. The results indicate that the tensile strength of the modified fibers slightly increases with the relative molecular mass of PEG. The main reason is that the increased PEG molecular mass facilitates the phase separation from PET, while PET crystallization acts as a physical cross-link.

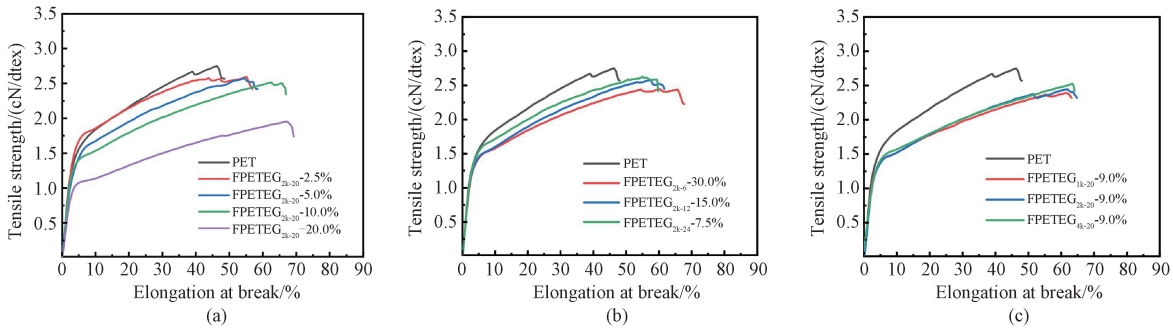

Fig. 9 Mechanical properties of modified PET fibers: (a) different amounts of masterbatches; (b) different types of masterbatches; (c) different relative molecular masses of masterbatches

2.8 Dyeing performance

To investigate how the masterbatch amounts and types affect fiber dyeability, fibers were dyed at 90 ℃ for 40 min. Their physical samples are shown in Fig. 10.

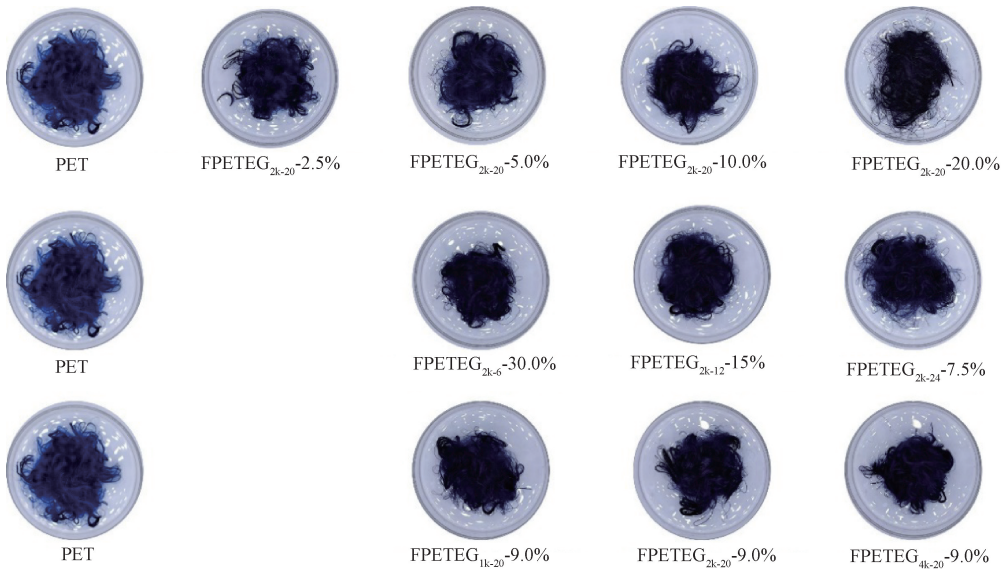

Fig. 10 Physical samples of low-temperature dyeing of PET fibers with disperse dyes

The *K/S* value is a key indicator of the dyeing depth. A higher *K/S* value indicates a deeper color[32]. Figure 11 illustrates the relationship between the *K/S* value and the low-temperature dyeing of PET fibers with disperse dyes at various temperatures for 40 min. The *K/S* values of the samples increase with increasing temperature. However, the rate of increase slows once the temperature reaches 110 ℃ due to saturation of the dyes in the fibers. For the modified fibers, the *K/S* value increases with a higher masterbatch content. This indicates a greater uptake of disperse dyes. This trend is consistent with the observed changes in sample crystallinity. Notably, for the sample with a PEG mass fraction of 4%, the color depth achieved at 90 ℃ is comparable to that of the pure PET sample dyed at 130 ℃.

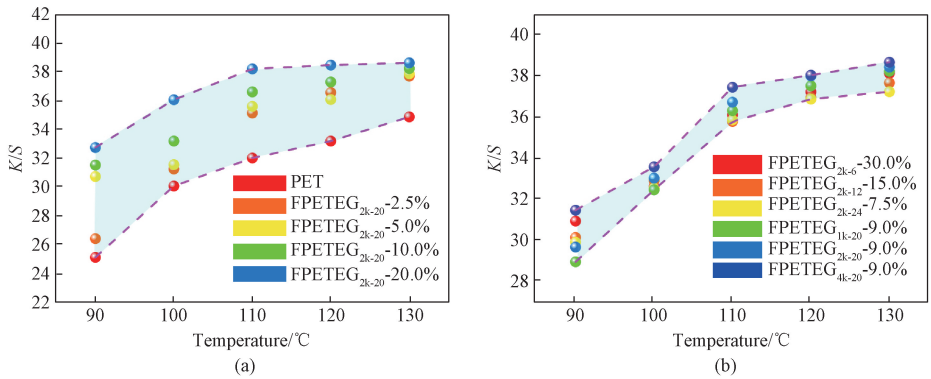

Fig. 11 *K/S* values of modified PET fibers at different dyeing temperatures: (a) different amounts of masterbatches; (b) different types of masterbatches

Figure 12 shows the dye-uptake of various modified PET fibers at different temperatures. As shown in Fig. 12(a), the dye-uptake of PET at 100 ℃ is only 63.21%. However, with the increase in masterbatch content, the dye-uptake gradually increases. The dye-uptake of FPETEG$_{2k\text{-}20}$-20.0% reaches 92.66% at 100 ℃. This is mainly because the addition of masterbatch increases the size of the amorphous region of the modified fiber, resulting in a looser stacking of lamellar crystals and thereby facilitating dye penetration. Moreover, the dye-uptake of FPETEG$_{2k\text{-}20}$-20.0% at 100 ℃ is comparable to that of PET at 130 ℃, indicating that atmospheric pressure boiling dyeing is achieved in this sample. Figure 12(b) shows the dye-uptake of modified fibers made from different types of masterbatches. FPETEG$_{2k\text{-}6}$-30.0% has the highest dye-uptake at the same PEG content. This indicates that a high proportion of low-modification masterbatch can effectively increase the dye-uptake of PET. Furthermore, the masterbatch prepared with higher relative molecular mass PEG significantly enhances the dyeability of PET, which is consistent with the SAXS characterization results.

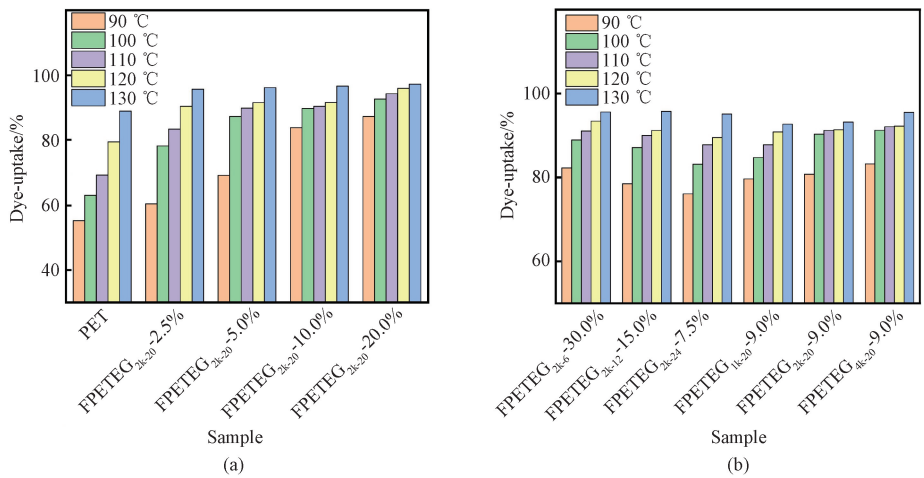

Fig. 12 Dye-uptake at different temperatures: (a) different amounts of masterbatches; (b) different types of masterbatches

The soap washing fastness (including staining and color change) of the modified PET fibers is shown in Table 5.

Table 5 Soap washing fastness of modified PET fibers

Sample	Grade of staining		Grade of color change
	PET	Cotton	
PET	4–5	5	4–5
FPETEG$_{2k\text{-}20}$-2.5%	4–5	4–5	4–5
FPETEG$_{2k\text{-}20}$-5.0%	4–5	4–5	4
FPETEG$_{2k\text{-}20}$-10.0%	4–5	4–5	4
FPETEG$_{2k\text{-}20}$-20.0%	4	4–5	3–4
FPETEG$_{2k\text{-}6}$-30.0%	4–5	4–5	4
FPETEG$_{2k\text{-}12}$-15.0%	4–5	4–5	4
FPETEG$_{2k\text{-}24}$-7.5%	4–5	4–5	4
FPETEG$_{1k\text{-}20}$-9.0%	4–5	4–5	4
FPETEG$_{2k\text{-}20}$-9.0%	4–5	4–5	4
FPETEG$_{4k\text{-}20}$-9.0%	4–5	4–5	4

The color fastness to staining for all samples is rated of grade 4 or higher, while the color fastness to color change is at grade 3–4 or higher. The FPETEG$_{2k\text{-}20}$-20.0% sample exhibits a reduced color fixation ability. This is due to the introduction of a large amount of PEG-modified masterbatch (at a mass fraction of 4%), which significantly disrupts the PET crystal structure. During low-temperature soaping, the dispersed dyes are more likely to migrate from the amorphous regions and diffuse into the adjacent fabric samples. Moreover, the dyes have a stronger affinity for the standard PET fabric than for the standard cotton fabric, resulting in a lower staining color fastness grade on the PET fabric[33]. No significant differences in the soap washing fastness are observed among the modified PET fibers.

3 Conclusions

To investigate the quantitative relationship between the amorphous region size and dyeing properties of PET fibers, PEG copolymerized modified PET was synthesized. By controlling the addition and relative molecular mass of PEG during copolymerization and masterbatch blending, the soft-hard segment distribution was modulated. The results indicate that the increased masterbatch content enhances hydrophilicity (e.g., a WCA of 52.40° for SPETEG$_{2k\text{-}20}$-20.0%) without damaging the original crystal lattice of PET. Although a higher masterbatch addition reduces the crystallinity and crystal size, and increases the amorphous region size (e.g., a crystallinity of 27.61% for FPETEG$_{2k\text{-}20}$-20.0%). Among different modification methods, using a low PEG modification content with high masterbatch addition most significantly reduces the crystallinity (28.15%), increases the interlamellar amorphous layer thickness, and

raises the lamellar inclination angle compared to pure PET, resulting in a looser crystal structure more conducive to dyeing. Masterbatches with higher relative molecular mass PEG are more effective in inducing phase separation and inhibiting lamellar crystal growth. The modified fibers exhibit a higher tensile strength than pure PET. Dyeing tests show that the dye-uptake at 100 ℃ increases from 63.21% to 92.66%, while all samples maintain a staining color fastness of grade 4 or higher and a color change fastness of 3 − 4 or higher after soap washing. This research provides an industrially viable solution for efficient, low-temperature, and low-energy dyeing of PET fibers.

References

[1] DISSANAYAKE L, JAYAKODY L N. Engineering microbes to bio-upcycle polyethylene terephthalate [J]. *Frontiers in Bioengineering and Biotechnology*, 2021, 9: 656465.

[2] SOUISSI M, KHIARI R, ZAAG M, et al. Ecological and cleaner process for dyeing bicomponent polyester filaments (PET/PTT) using ecological carriers: analysis of dyeing performance [J]. *RSC Advances*, 2021, 11 (42): 25830-25840.

[3] FU C F, GU L X. Structures and properties of easily dyeable copolyesters and their fibers respectively modified by three kinds of diols[J]. *Journal of Applied Polymer Science*, 2013, 128 (6): 3964-3973.

[4] HASHIM S, XUE D, BI X Y, et al. Influence of lawsone dye on surface properties of polyethylene terephthalate fabric[J]. *Journal of Donghua University (English Edition)*, 2025, 42 (1): 71-77.

[5] SOUISSI M, KHIARI R, ABDELWAHEB M, et al. Kinetics study of dyeing bicomponent polyester textiles (PET/PTT) using environmentally friendly carriers [J]. *RSC Advances*, 2022, 12(4): 2361-2374.

[6] SASAKI K, HIROGAKI K, TABATA I, et al. Supercritical fluid dyeing of polyester fabrics using polymeric nanofibers loaded with disperse dye[J]. *The Journal of Supercritical Fluids*, 2024, 211: 106289.

[7] HSIAO K J, KUO J L, TANG J W, et al. Physics and kinetics of alkaline hydrolysis of cationic dyeable poly (ethylene terephthalate) (CDPET) and polyethylene glycol (PEG)-modified CDPET polymers: effects of dimethyl 5-sulfoisophthalate sodium salt/PEG content and the number-average molecular weight of the PEG [J]. *Journal of Applied Polymer Science*, 2005, 98(2): 550-556.

[8] MAMUN KABIR S M, RAHMAN M M, HONG I, et al. Comparative characterization and dyeing properties of poly (ethylene terephthalate-co-polyethylene glycol) fibers and poly (ethylene terephthalate) fibers[J]. *Polymer*, 2024, 311: 127488.

[9] GE T J, WANG M Y, HE X F, et al. Synthesis and characterization of poly (butylene glycol adipate-co-terephthalate/diphenylsilanediol adipate-co-terephthalate) copolyester [J]. *Polymers*, 2024, 16(8): 1122.

[10] HUANG Z, BAO J N, ZHANG X M, et al. New insights in structures, properties, and rheological behaviors of cationic dyeable polyesters [J]. *Industrial & Engineering Chemistry Research*, 2023, 62 (36): 14648-14656.

[11] ZHOU R, WANG X L, HUANG L Q, et al. Poly (ethylene terephthalate) copolyesters and fibers modified with NPG and SIPE for improved hydrophilicity and dyeability[J]. *The Journal of the Textile Institute*, 2017, 108 (11): 1949-1956.

[12] ZHANG S M, WU Y H, YANG H B, et al. Preparing cationic dyeable polyamide 6 filaments by combining the masterbatch technique with melt copolymerization[J]. *Textile Research Journal*, 2022, 92(3/4): 511-524.

[13] RWEI S P, LIN W P, WANG J F. Synthesis and characterization of biodegradable and weather-durable PET/PEG/NDC copolymers[J]. *Colloid and Polymer Science*, 2012, 290: 1381-1392.

[14] GAN Z Y, FENG Y B, YANG J J, et al. The copolymerization of flexible poly (ethylene terephthalate)-poly(ethylene oxide terephthalate) poly(ether ester)s and brittle polylactic acid: balanced mechanical properties and potential biodegradability [J]. *Reactive and Functional Polymers*, 2022, 180: 105392.

[15] LU H, WANG H L, ZHENG A N, et al. Hybrid poly (ethylene terephthalate)/silica nanocomposites prepared by in situ polymerization[J]. *Polymer Composites*, 2007, 28(1): 42-46.

[16] LI X, LIU R, ZHONG L, et al. Antielectrostatic poly (ether ester) block copolymer of poly (ethylene terephthalate-co-isophthalate)-poly (ethylene glycol) [J]. *Journal of Applied Polymer Science*, 2003, 89(6): 1696-1701.

[17] GOLMOHAMMADI N, BOLAND-HEMMAT M, BARAHMAND S, et al. Coarse-grained molecular dynamics simulations of poly(ethylene terephthalate) [J]. *The Journal of Chemical Physics*, 2020, 152(11): 114901.

[18] PENG Y, WANG Y, DAN Y D, et al. Silicon-linked polyethylene glycol-polyethylene terephthalate (PEG-PET) nanostructures loaded with Eu^{3+}-complexes for hybrid luminescent PET materials[J]. *Polymer Composites*, 2024, 45

(2): 999-1011.
[19] JI P, LU D P, ZhANG S M, et al. Modification of poly (ethylene 2,5-furandicarboxylate) with poly (ethylene glycol) for biodegradable copolyesters with good mechanical properties and spinnability [J]. *Polymers*, 2019, 11(12): 2105.
[20] SUN L N, HUANG L Q, WANG X L, et al. Synthesis and structural characterization of sequential structure and crystallization properties for hydrophilic modified polyester[J]. *Polymers*, 2020, 12(8): 1733.
[21] GÜNGÖÖR ERTUĞRAL T, ALKAN C. Synthesis of thermally protective PET-PEG multiblock copolymers as food packaging materials [J]. *Polymers and Polymer Composites*, 2021, 29(Sup. 9): S1125-S1133.
[22] KANG C S, YOON H J, HONG C H, et al. Synthesis of hydrophilic copolyesters and the characterization of their moisture-related cooling properties[J]. *Fibers and Polymers*, 2015, 16(12): 2513-2518.
[23] SHARMA P R, VARMA A J. Thermal stability of cellulose and their nanoparticles: effect of incremental increases in carboxyl and aldehyde groups[J]. *Carbohydrate Polymers*, 2014, 114: 339-343.
[24] PAN Z Q, ZHU L Q. Synthesis of a siloxane oligomer containing ether bond for promoting the adhesion between addition-cure silicone rubber and polycarbonate (PC)[J]. *Silicon*, 2023, 15(10): 4425-4437.
[25] SUN N, ZOU J X, ZHANG Y, et al. The competition mechanism of orientation and disorientation of PET chains during spinning based on the pre-oriented polyester industrial yarns[J]. *Polymer*, 2024, 300: 126991.
[26] SHARMA K, BRAUN O, TRITSCH S, et al. 2D Raman, ATR-FTIR, WAXD, SAXS and DSC data of PET mono-and PET/PA6 bicomponent filaments[J]. *Data in Brief*, 2021, 38: 107416.
[27] PERRET E, HUFENUS R. Fitting of 2D WAXD data: mesophases in polymer fibers[J]. *Data in Brief*, 2021, 39: 107466.
[28] PERRET E, CHEN K, BRAUN O, et al. Radial gradients in PET monofilaments: a Raman mapping and SAXS tomography study [J]. *Polymer*, 2022, 238: 124422.
[29] LIU Y T, YIN L X, ZHAO H R, et al. Strain-induced structural evolution during drawing of poly (ethylene terephthalate) fiber at different temperatures by in situ synchrotron SAXS and WAXD[J]. *Polymer*, 2017, 119: 185-194.
[30] STRIBECK N, FAKIROV S, APOSTOLOV A A, et al. Deformation behavior of PET, PBT and PBT-based thermoplastic elastomers as revealed by SAXS from synchrotron[J]. *Macromolecular Chemistry and Physics*, 2003, 204(7): 1000-1013.
[31] MA J P, YU L, CHEN S, et al. Structure-property evolution of poly (ethylene terephthalate) fibers in industrialized process under complex coupling of stress and temperature field[J]. *Macromolecules*, 2019, 52(2): 565-574.
[32] OMAR A Z, EL-RAHMAN M A, EL-SADANY S K, et al. Synthesis of novel bisazo disperse dyes: spectroscopic characterization, DFT study and dyeing of polyester[J]. *Dyes and Pigments*, 2021, 196: 109831.
[33] PALUSZKIEWICZ J, GRZELAKOWSKA A, RUTOWICZ J. Diesters of monoimide of perylene-3,4,9,10-tetracarboxylic acid: synthesis, characterization, and application for dyeing polyester fibre, polystyrene, and poly (methyl methacrylate) films [J]. *Luminescence*, 2024, 39(9): e4890.

PEG 改性 PET 母粒的合成：基于相区尺寸调控制备低温易染、高色牢度 PET 纤维

肖永兵[1]，徐朝晨[1]，沈午枫[1]，张圣明[1]，陈向玲[1]，吉　鹏[2*]，王朝生[1]，王华平[1]

1. 东华大学 先进纤维材料全国重点实验室 东华大学材料科学与工程学院，上海 201620

2. 东华大学 纺织科技创新中心，上海 201620

摘　要：聚对苯二甲酸乙二醇酯（polyethylene terephthalate，PET）纤维是化学纤维中用量最大的一类，被广泛应用于多种领域。然而，PET 纤维的染色需要在高温高压（130 ℃、0.2 MPa）下进行，使染色过程消耗大量能源。现有研究表明，PET 的染色性能与无定形区的大小直接相关，该结构特征决定了染色的外部条件。该文通过使用不同数均分子量及不同添加量的聚乙二醇（polyethylene glycol，PEG），合成了一系列易染母粒（PETEG）。利用母粒法调控 PET 纤维的无定形区相区尺寸。从母粒添加量、添加种类，以及 PEG 相对分子质量等方面，探究了无定形区相区尺寸与染色性能之间的关系。结果表明，添加质量分数为 20%的 PEG-2000 改性母粒制备的纤维样品，其结晶片层厚度较小（5.59 nm），而片层间无定形层厚度较大（6.43 nm）。长周期和片层倾角增大，致使结构更为疏松，这使得小分子染料更容易扩散进入纤维内部。添加母粒后，分散染料在 100 ℃时的上染率可从 63.21%提升至 92.66%。上染率随着 PEG 的相对分子质量及母粒添加量的增加而上升，染色后纤维的沾色牢度均达到 4 级及以上。该研究通过开发简单的母粒实现了 PET 纤维的常压染色，为 PET 纤维高效、低温、低能耗的染色应用提供了一种可工业化实施的解决方案。

关键词：聚对苯二甲酸乙二醇酯（PET）纤维；聚乙二醇（PEG）；低温染色；相区尺寸；上染率；色牢度